Extended Abstracts of the 2016 International Conference on Solid State Devices and Materials, Tsukuba, 2016, pp85-86

B-3-01

A Physics-Based Compact Model of Resistive Switching for Bi-layered TaO_X-RRAM

Yudi Zhao, *Peng Huang, Junjie Hu, Xiaoyan Liu, *Jinfeng Kang
Institute of Microelectronics, Peking University, 100871 Beijing, China *phwang@pku.edu.cn, kangjf@pku.edu.cn

Abstract

A physics-based compact model is proposed to quantify the DC and AC switching characteristics of bi-layered Ta_2O_5/TaO_X RRAM. In the model, the evolution of conductive filament consisting of oxygen vacancies and TaO_2, the resistance of TaO_X base layer correlated with oxygen content and Schottky barrier between Ta_2O_5/TaO_X are physically involved. The model can reproduce the main features of bi-layred TaO_X-RRAM under static and transient operations. The model is verified and calibrated by the measured data, and the excellent agreements between model and experiments show its potential in circuit simulation.

1. Introduction

TaO_X-based resistance random access memory (RRAM) has demonstrated great potential for future nonvolatile memories given its highly reliable resistive switching (RS) behaviors such as robust endurance (>10^{12} cycles) and excellent data retention property [1-10]. A typical device structure of TaO_X-based RRAM is a bi-layered Ta_2O_5/TaO_X stack sandwiched between two electrodes. The Ta_2O_5 layer is the resistive switching layer (RSL) and the oxygen deficient TaO_X base layer (TBL) acts as an oxygen reservoir. Several modeling studies have been reported to quantitatively describe RS behaviors of TaO_X-based RRAM, but the compact model connect RS with the underlying physics of the conductive filament (CF) evolution and the interaction between RSL/TBL is still limited [4-8]. In this work, a physics-based compact model of bi-layered TaO_X-based RRAM is presented. The physical processes associated with RS behaviors including CF evolution, TBL resistance modified by oxygen content and Schottky barrier effect between RSL/TBL are involved. The metallic and electron hopping transport, heat conduction and parasite effects are also included in the model. The model is verified and calibrated by the experiments under both DC and AC operations. The model can be utilized in circuit simulation for design optimization.

2. Physical Mechanism

Fig. 1 shows the physical processes in a bi-layered TaO_X-RRAM [10]. During SET process, V_O and TaO_2 are generated by ionizing O^{2-} from Ta_2O_5 under electric field and thermal effects. The generated O^{2-} hops in RSL and then drift into TBL. TBL can take redox reactions with O^{2-} and store part of O^{2-} as lattice oxygen. When CF consisting of V_O and TaO_2 connects top electrode and TBL, the device is switched to low resistance state (LRS). During RESET, O^{2-} is released by TBL to recombine with V_O or react with TaO_2 in RSL, leading to the rupture of CF. The device is then switched to high resistance state (HRS). The energy relationships of Ta-O and migration of O^{2-} in RSL/TBL are shown in **Fig. 2**, and equations describing these physical processes are also listed.

3. Compact model

The RS behaviors are associated with the CF evolution similar to the HfO_X-based RRAM [8]. However, in bi-layered TaO_X-based RRAM, TBL with variable resistance and Schottky barrier also contribute to the RS property. The CF evolution can be investigated with a developed atomic Monte-Carlo simulator of bi-layered TaO_X-based RRAM [10]. During RESET, the gap distance x determines HRS resistance and the increase of x is decided by the slowest process in (1)~(3) as shown in **Fig. 3**. During SET, as shown in **Fig. 4**, LRS is determined by x and CF width w. dx/dt and dw/dt are associated with G-R and P-T, whose ratio is decided by electric field and temperature in equation (11). I-V characteristics of LRS and HRS can be modeled as shown in **Fig. 5**. The resistivity of TBL is modeled by dynamically counting oxygen content in TBL during RS and is calibrated with experiment as shown in **Fig. 6**. **Fig. 7** shows the Schottky barrier model between RSL/TBL. The Schottky barrier is modified by V_O doping density in RSL and Fermi-level pinning effect. The parameters used in the model are listed in Table I.

4. Results and discussions

The model is verified and calibrated with experiments in [4] and [9]. Modeled and measured DC I-V curves are shown in **Fig. 8**, where Schottky barrier can be obviously observed through asymmetric HRS [9]. Excellent agreements are achieved between model and measurements. **Fig. 9** shows a case with slight Schottky barrier and the corresponding temperature voltage relationships, which further verify the validity of the model [4]. **Fig. 10** shows the impacts of V_O ratio in CF on SET voltage. The results indicate that small V_O ratio leads to large SET voltage, which is more obvious under larger gap distance. The impacts of TBL resistance on SET are shown in **Fig. 11**. Large TBL resistance leads to obvious self-compliance behaviors. The parasite resistance and capacitance are also considered as shown in **Fig. 12**. The calculated and measured transient response is shown in **Fig. 13**. **Fig. 14** shows the pulse switching property.

5. Conclusions

A compact model of bi-layered TaO_X-based RRAM is developed based on the physical processes during RS. The compact model is verified by experiments under DC and AC operations and excellent agreements are achieved between model predictions and experiments. The model can be used in RRAM optimization design and circuit simulation.

Acknowledgements

This work is supported by NSFC (61421005, 61334007).

References: [1] M-J. Lee et al., Nat. Mat. 2011, 10, 625-630. [2] Z. Wei et al., IEDM 2011, 721-724. [3] L.Goux et al., VLSI 2014, 162-163. [4] S. Kim et al. Sci. Rep. 2013, 3, 1680. [5] F. O. Hatem et al., Semicond. Sci. Technol., 2015, 30, 115009. [6] J. P. Strachan et al., Trans. Electron Devices, 2013, 60, 2194. [7] A. Simon et al., ISCAS 2014, 1420-1423. [8] P. Huang et al., Trans. Electron Devices, 2013, 60, 4091-4097. [9] K. M. Kim et al., Adv. Funct. Mater. 2015, 25, 1527-1534. [10] Y. D. Zhao et al., Trans. Electron Devices, 2016, 63, 1524-1532.

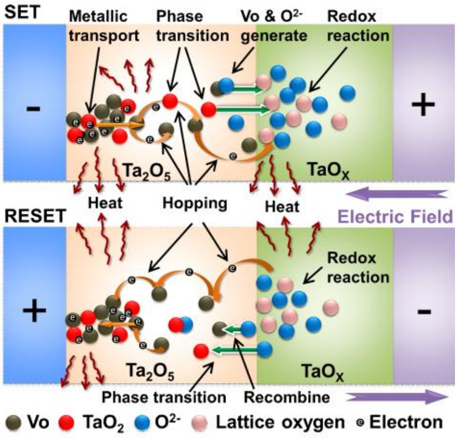

Fig. 1 Schematic physical processes in bi-layered TaO_X-RRAM.

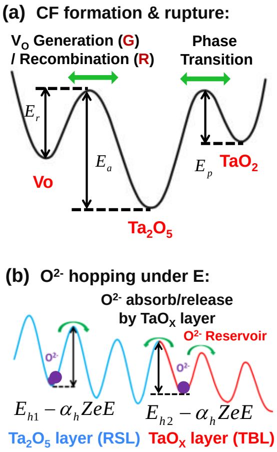

$$Ta_2O_5 + 2e^- \leftrightarrow 2TaO_2 + O^{2-} \quad (1)$$

$$P_{a1}(T,dt) = f dt \exp(-E_a / k_B T) \quad (2)$$

$$P_p(T,dt) = f dt \exp(-E_p / k_B T) \quad (3)$$

Phase Transition (P-T)

$$O_L \leftrightarrow V_O^{2+} + O^{2-} \quad (4)$$

V_O Generation /Recombination (G-R)

G: $P_{a2}(E,T,dt) = f dt \exp(-(E_a - \alpha_a ZeE) / k_B T)$ (5)

R: $P_r(T,dt) = f dt \exp(-E_r / k_B T)$ (6)

$$P_h(E,T,dt) = f dt \exp(-(E_h - \alpha_h ZeE) / k_B T) \quad (7)$$

$P_{a1} \sim P_h$ the probabilities of the physical processes, f the vibration frequency, $E_a \sim E_h$ the activation energies, E the local electric field, Z the charge number, α_a & α_h the enhancement factor of electric filed, T the local temperature.

Fig. 2 The energy relationships of the physical processes and the corresponding equations used in the model.

Table I Parameters

Parameters	Value
f	10^{13} Hz
E_a, E_r, E_p	1.3,1.0,0.8 eV
E_{h1}, E_{h2}	1.5,1.75 eV
α_a, α_h	0.75 nm
a	0.25 nm
Δw	0.5 nm
x_T	0.4 nm^{-1}
V_T	0.4 V^{-1}
R_{th}	5×10^5 k/W
A^*	10^7 $Am^{-2}K^{-2}$
φ_{B0}	0.5 V
V_b	0.1 V
n_S	10^{24} m^{-3}
ε	15 ε_0
C_P	2 pF
R_C	20 Ω

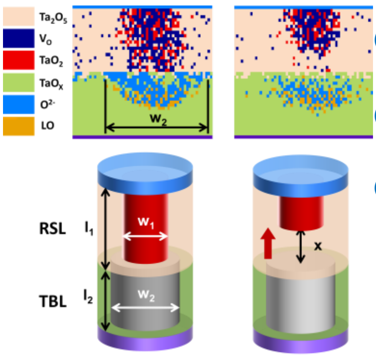

RESET

(1) O^{2-} hopping from TBL to RSL dominant (8)

$$\frac{dx}{dt} = af\exp(-\frac{E_{h2}}{k_BT})\sinh(\frac{\alpha_h ZeE_r}{k_BT})(\frac{w_2}{w_1})^2$$

(2) O^{2-} hopping in RSL dominant (9)

$$\frac{dx}{dt} = af\exp(-\frac{E_{h1}}{k_BT})\sinh(\frac{\alpha_h ZeE_t}{k_BT})$$

(3) G-R and P-T dominant (10)

$$\frac{dx}{dt} = af(\lambda\exp(-\frac{E_r}{k_BT}) + (1-\lambda)\exp(-\frac{E_p}{k_BT}))$$

G-R P-T

w_2: width of oxygen distribution in TBL

Ratio factor: $\lambda(E,T) = \frac{1}{\exp(-\frac{\alpha_a ZeE_{SET}}{k_BT}) + 1}$ (11)

Fig. 3 RESET process is modeled based on the simulated CF evolution. The increase of gap distance (x) is determined by processes (1)~(3).

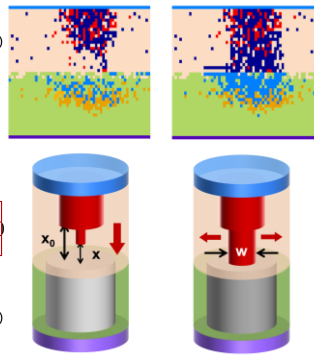

SET

(1) Thin CF grow to connect electrode and TBL (12)

$$\frac{dx}{dt} = -af(\lambda\exp(-\frac{E_{a2}-\alpha_a ZeE}{k_BT}) + (1-\lambda)\exp(-\frac{E_{a1}-\alpha_a ZeE}{k_BT}))dt$$

G-R P-T

(2) CF expand in width (13)

$$\frac{dw}{dt} = f(\Delta w + \frac{\Delta w^2}{2w})(\lambda\exp(-\frac{E_{a2}-\alpha_a ZeE}{k_BT}) + (1-\lambda)\exp(-\frac{E_{a1}-\alpha_a ZeE}{k_BT}))$$

G-R P-T

Temperature Model: $T = T_0 + IVR_{th}$ (14)

T_0 the ambient temperature, R_{th} the effective thermal resistance, a the lattice distance, E_r / E_t the electric field of RSL/TBL, Δw the effective CF expands width.

Fig. 4 SET process is modeled based on the simulated CF revolution and is decided by gap distance (x) and CF width (w).

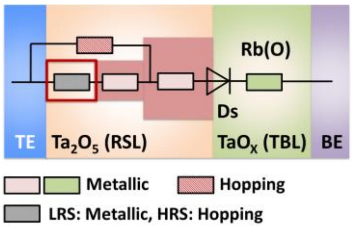

Metallic: $I = Vw^2/(4l\rho)$ (15)

Hopping: $I = \pi(\frac{w}{2})^2 J_0 \exp(-\frac{x}{x_T}/)\sinh(\frac{V}{V_T})$ (16)

x_T and V_T are the characteristic length and voltage of hopping.

Fig. 5 Equivalent circuit of conduction.

Generated O^{2-} during switching:

$$N(O^{2-}) = N(V_O) + N(TaO_2)$$

$V > 0$, (17)

$$N(O^{2-}) = (\pi(\frac{w_1}{2})^2(l_1 - x))/a^3$$

$V < 0$, (18)

$$N(O^{2-}) = (\pi(\frac{w_1}{2})^2(l_1 - x_0) + \pi(\frac{w}{2})^2(x_0 - x))/a^3$$

Oxygen content in TBL:

$$\frac{O}{Ta+O} = \frac{N(O^{2-}) + yN(TaOy)}{(1+y)N(TaOy)} \quad (19)$$

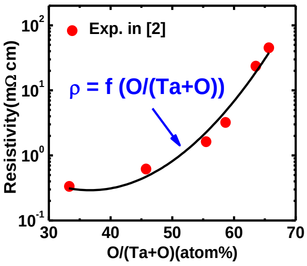

Fig. 6 Dependence of TBL resistivity on oxygen content. In equation (20), TBL is set to TaOy initially.

Current with Schottky barrier:

$$I = I_0(\exp(q(V - IR_{eq})/nkT) - 1) \quad (20)$$

$$I_0 = AA^*T^2\exp(-q(\phi_{B0} - \Delta\phi_B)/kT) \quad (21)$$

Barrier height modified by doping in RSL and Fermi-level pinning effect:

$$\phi_{B0} = pin\cdot\phi_{B0}\cdot x/x_0 \quad (22)$$

Image force lowering effect (small):

$$\Delta\phi_B = (q^3 n_s(V_{SB} - (V - IR_{eq}))/8\pi^2\varepsilon^3)^{1/4} \quad (23)$$

R_{eq} the device equivalent resistance except Schottky barrier, V_{SB} the built in potential, of the physical processes, N_s the RSL charge density, pin the pinning factor.

Fig. 7 The Schottky barrier model between RSL/TBL.

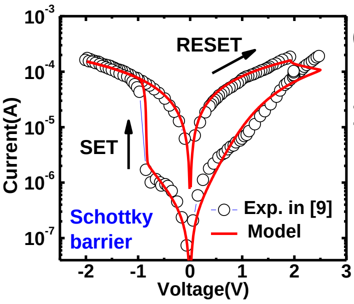

Fig. 8 Modeled DC I-V curve and its comparison with experiment.

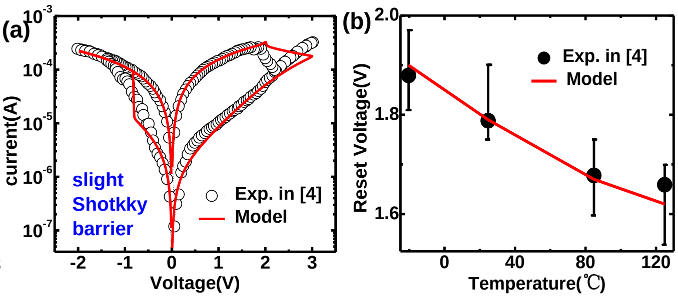

Fig. 9 (a) I-V curve with slight Schottky barrier and (b) corresponding temperature-voltage relationships.

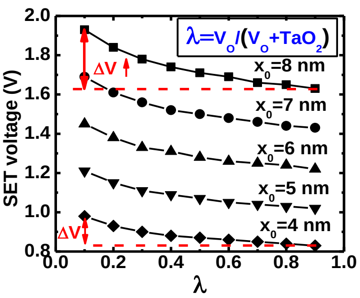

Fig. 10 The impacts of V_O ratio in CF on SET voltage.

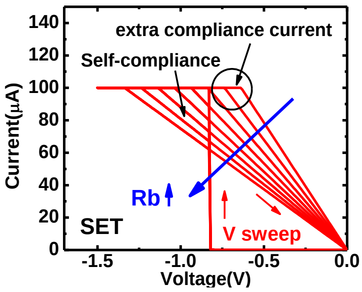

Fig. 11 The increase of TBL resistance leads to obvious self-compliance.

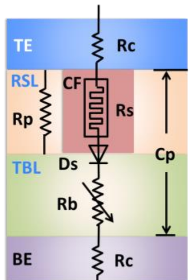

Fig. 12 Equivalent circuit with parasitic effects.

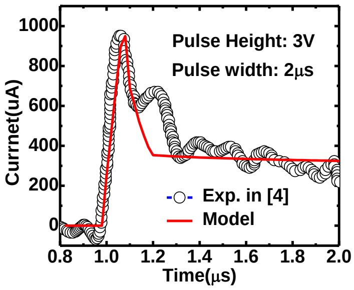

Fig. 13 Transient response during RESET process.

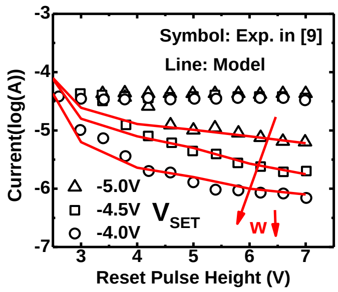

Fig. 14 Pulse switching property with 500 ns RESET pulse width.